Available online at www.sciencedirect.com

ScienceDirect

Geochimica et Cosmochimica Acta 120 (2013) 1–16

Geochimica et Cosmochimica Acta

www.elsevier.com/locate/gca

Magnesium isotopic composition of the Moon

Fatemeh Sedaghatpour [a,1], Fang-Zhen Teng [a,*], Yang Liu [b,2], Derek W.G. Sears [c,3], Lawrence A. Taylor [b]

[a] *Isotope Laboratory, Department of Geosciences and Arkansas Center for Space and Planetary Sciences, University of Arkansas, Fayetteville, AR 72701, USA*

[b] *Planetary Geosciences Institute, Department of Earth and Planetary Sciences, University of Tennessee, Knoxville, TN 37996, USA*

[c] *Department of Chemistry and Biochemistry and Arkansas Center for Space and Planetary Sciences, University of Arkansas, Fayetteville, AR 72701, USA*

Received 9 December 2012; accepted in revised form 20 June 2013; available online 8 July 2013

Abstract

The Mg isotopic compositions of 47 well-characterized lunar samples, including mare basalts, highland rocks, regolith breccias, and mare and highland soils were measured to address the behavior of Mg isotopes during lunar magmatic differentiation, constrain the Mg isotopic composition of the Moon, and evaluate the degree of Mg isotopic fractionation between planetary bodies. The δ^{26}Mg values range from -0.61 ± 0.03‰ to 0.02 ± 0.06‰ in 22 mare basalts, from -0.34 ± 0.04‰ to -0.18 ± 0.06‰ in 3 highland rocks, from -0.33 ± 0.05‰ to -0.14 ± 0.08‰ in 7 regolith breccias, from -0.23 ± 0.05‰ to -0.14 ± 0.07‰ in 6 highland soils, and from -0.41 ± 0.05‰ to -0.20 ± 0.09‰ in 9 mare soils. The limited Mg isotopic variation among bulk mare and highland soils and regolith breccias indicates negligible Mg isotope fractionation by lunar surface processes. By contrast, the large Mg isotopic fractionation between low-Ti and high-Ti basalts suggests the source heterogeneity produced during fractional crystallization of the lunar magma ocean, with ilmenite having lighter Mg isotopic compositions than olivine and pyroxene. Overall, the Moon has a weighted average Mg isotopic composition (δ^{26}Mg = -0.26 ± 0.16‰) indistinguishable from the Earth (δ^{26}Mg = -0.25 ± 0.07‰) and chondrites (δ^{26}Mg = -0.28 ± 0.06‰), suggesting homogeneous Mg isotopic distribution in the solar system and the lack of Mg isotope fractionation during the Moon-forming giant impact.

1. INTRODUCTION

Isotopic studies of terrestrial and lunar samples can provide insight into the complex processes that govern planetary accretion and differentiation. For instance, despite the large variation of oxygen isotopes in the solar system, the Earth and the Moon have identical O isotopic compositions (Clayton et al., 1973; Wiechert et al., 2001; Spicuzza et al., 2007; Hallis et al., 2010; Liu et al., 2010a), suggesting that materials in the proto-Moon and proto-Earth were from the same sources or well-mixed during the giant impact (Wiechert et al., 2001; Pahlevan and Stevenson, 2007).

Magnesium is a moderately refractory element in the solar system, with a condensation temperature of ~1400 K (Lodders, 2003). In addition to the non-mass-dependent isotope anomalies produced by the decay of short-lived ^{26}Al to ^{26}Mg (Lee et al., 1977), Mg isotopes can also fractionate mass dependently at high temperatures during condensation and evaporation processes, as observed from calcium–aluminum-rich inclusions (CAIs) (e.g., Clayton

* Corresponding author. Present address: Isotope Laboratory, Department of Earth and Space Sciences, University of Washington, Seattle, WA 98195, USA. Tel.: +1 206 543 7615.

E-mail address: fteng@u.washington.edu (F.-Z. Teng).

[1] Present address: Department of Earth and Planetary Sciences, Harvard University, 20 Oxford Street, Cambridge, MA 02138.

[2] Present address: Jet Propulsion Laboratory, California Institute of Technology, Pasadena, CA 91109, USA.

[3] Present address: Space Science and Astrobiology Division, MS245-3, NASA Ames Research Center, Moffett Field, Mountain View, CA 94035, USA.

0016-7037/$ - see front matter © 2013 Elsevier Ltd. All rights reserved.
http://dx.doi.org/10.1016/j.gca.2013.06.026

and Mayeda, 1977; Wasserburg et al., 1977; Lee et al., 1979; Niederer and Papanastassiou, 1984; Niederer et al., 1985; Clayton et al., 1988) and chondrules (Galy et al., 2000; Young et al., 2002), and as shown by experimental and theoretical studies (Davis et al., 1990; Richter et al., 2002, 2007). Knowledge of Mg isotopic compositions of terrestrial and extraterrestrial materials, therefore, can potentially be used to study the origin, formation, and differentiation of planetary objects (Richter et al., 2002; Young et al., 2002; Norman et al., 2006; Teng et al., 2007, 2010; Wiechert and Halliday, 2007). For example, Wiechert and Halliday (2007) found the Earth has heavy Mg isotopic compositions relative to chondrites. They interpreted the Mg isotope heterogeneity in the solar system as reflecting the physical separation and sorting of the chondrules and CAIs in the proto-planetary disk. However, more recent comprehensive studies on terrestrial basalts, komatiites and peridotites indicate that the Earth has a Mg isotopic composition indistinguishable from chondrites within uncertainties (Teng et al., 2007, 2010; Handler et al., 2009; Yang et al., 2009; Bourdon et al., 2010; Chakrabarti and Jacobsen, 2010; Dauphas et al., 2010; Schiller et al., 2010; Huang et al., 2011; Liu et al., 2011; Pogge von Strandmann et al., 2011; Xiao et al., 2013).

Studies of the Mg isotopic composition of the Moon can shed light on Mg isotopic distribution in the solar system. Compared to the Earth and chondrites, our understanding of the Mg isotopic composition of the Moon is still a subject of controversy. *In-situ* analyses reveal homogeneous Mg isotopic compositions in lunar mare basalts, glasses and impact melts, similar to the Earth and chondrites at $\sim \pm 0.2‰\ amu^{-1}$ (2SD) (Warren et al., 2005; Norman et al., 2006). By contrast, Wiechert and Halliday (2007), by using solution method MC-ICPMS with a higher precision ($\sim \pm 0.05‰\ amu^{-1}$, 2SD), found that Mg isotopic composition of the Moon is $\sim 0.09‰\ amu^{-1}$ heavier than that of the Earth, and both the Earth and Moon are heavier than chondrites. With similar precision, Chakrabarti and Jacobsen (2010) reported that the Moon has an identical Mg isotopic composition to chondrites. Nonetheless, the values for most terrestrial and chondrite samples reported by Chakrabarti and Jacobsen (2010) and Wiechert and Halliday (2007) are different from those reported by other groups (Teng et al., 2007, 2010; Handler et al., 2009; Yang et al., 2009; Bourdon et al., 2010; Dauphas et al., 2010; Schiller et al., 2010; Huang et al., 2011; Liu et al., 2011; Pogge von Strandmann et al., 2011; Xiao et al., 2013).

To better constrain the Mg isotopic composition of the Moon, understand behaviors of Mg isotopes during the lunar-forming giant impact and lunar magmatism, and evaluate the extent of Mg isotopic heterogeneity in the solar system, we have studied 47 well-characterized samples from all major types of lunar rocks returned by the Apollo 11, 12, 14, 15, 16 and 17 missions. Our results show limited Mg isotopic variation in lunar highland rocks, breccias, soil samples and low-Ti basalts, which are similar to terrestrial basalts and chondrites. By contrast, high-Ti basalts tend to have light Mg isotopic compositions, which may reflect the source heterogeneity produced during differentiation of the lunar magma ocean (LMO).

2. SAMPLES

The samples investigated in this study are from the same collection as those studied by Batchelor et al. (1997) and some of those studied for oxygen and iron isotopes by Spicuzza et al. (2007) and Liu et al. (2010a). They represent a diverse spectrum of sample types including highland rocks, mare volcanic rocks, regolith breccias, and mare and highland lunar soils, with a broad range of lunar geological settings and geochemical properties (Fig. 1 and Table 1). Petrography, mineralogy, and major- and trace-element compositions of these samples are available in the lunar sample compendium (Meyer, 2004–2011).

2.1. Highland rocks

Highland rocks are classified into four major groups: ferroan-anorthosites, Mg-rich suite rocks, gabbros/norites, and alkali-suite rocks (e.g., Lucey et al., 2006). The lunar highlands, decidedly older than the maria, were subjected to heavy bombardment, and primary igneous rocks were broken, mixed, and melted into various types of breccias. Three highland rocks from Apollo 14 and 16 were analyzed for Mg isotopes in this study (Table 1).

2.2. Mare volcanic rocks

Mare volcanic rocks include various types of basalts that were derived from partial melting of cumulates originally formed by the LMO crystallization. On the basis of the bulk-rock TiO_2 content, mare basalts are classified into high-Ti basalts (HT) (>6 wt.% TiO_2), low-Ti (LT) basalts (1.5–6 wt.% TiO_2), and very low-Ti (VLT) basalts (<1.5 wt.% TiO_2) (Neal and Taylor, 1992). The basalt samples from the Apollo 12 and 15 missions are mostly low-Ti basalts, whereas those from the Apollo 11 and 17 missions consist mainly of high-Ti basalts. Based on mineralogy, and major- and trace-element compositions, Apollo 12 basalts

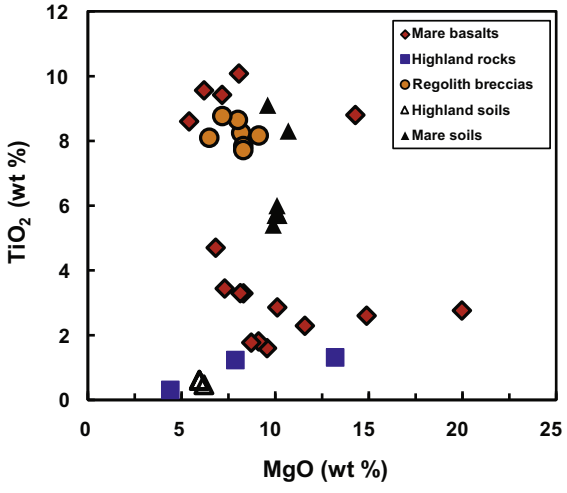

Fig. 1. Variation of TiO_2 versus MgO contents for lunar samples studied here. Data are reported in Table 1.

Table 1
Chemical compositions of lunar samples investigated in this study.

Sample	MgO	SiO_2	TiO_2	FeO	CaO
Volcanic rocks:					
Mare basalts					
10020, 222 High-Ti basalt	7.7	40.2	10.6	18.9	12.0
10049, 89 High-Ti, High-K basalt	7.3	41.0	9.6	18.2	9.9
12002, 240 Low-Ti basalt	14.8	44.0	2.6	21.8	8.2
12005, 46 Low-Ti basalt	19.9	41.5	2.7	22.2	6.3
12051, 48 Low-Ti basalt	7.0	45.7	4.5	20.1	11.2
12011, 25 Low-Ti basalt	8.7	46.6	3.2	19.4	10.6
12021, 574 Low-Ti basalt	7.2	46.5	3.5	19.2	11.5
12052, 330 Low-Ti basalt	8.5	45.8	3.2	20.1	11.0
15058, 239 Low-Ti basalt	9.5	47.7	1.8	19.6	10.2
15075, 52 Low-Ti basalt	NA	NA	NA	NA	NA
15475, 187 Low-Ti basalt	8.7	48.3	1.7	19.8	10.3
15499, 13 Low-Ti basalt	9.1	47.7	1.8	20.2	10.3
15016, 221 Low-Ti basalt	11.1	44.1	2.3	22.0	9.4
15555 Low-Ti basalt	11.1	44.15	2.2	22.3	9.4
70035, 9 High-Ti basalt	9.9	37.8	13.0	18.5	10.0
71539, 17 High-Ti basalt	5.4	NA	8.6	19.1	12.1
75015, 1 High-Ti basalt	5.8	41.9	9.2	19.9	11.9
70215, 322 High-Ti basalt	8.7	37.9	12.9	19.7	10.8
75075, 171 High-Ti basalt	9.6	38.1	13.3	18.8	10.3
74255, 185 High-Ti basalt	10.7	38.4	12.5	17.8	10.3
70017, 524 High-Ti basalt	9.8	38.2	13.3	18.5	10.4
Mare pyroclastic glasses					
74220, 758[a]	14.4	38.5	8.8	22.0	7.7
Highland rocks					
14310, 631 Impact melt	7.8	47.1	1.2	8.3	12.3
60315, 30 Coherent poikilitic impact melt	13.2	46.5	1.3	9.3	10.2
68415, 200 Clast-poor impact melt	4.4	45.5	0.3	4.1	16.3
Regolith breccias					
10018, 101	8.1	42.4	8.2	16.4	11.9
10019, 85	6.4	42.4	8.1	16.3	14.0
10021, 90	8.2	43.2	7.7	16.0	12.1
10046, 231	9.1	44.0	8.1	16.0	13.0
10048, 198	7.1	40.4	8.7	16.3	11.0
10060, 136	8.0	42.1	8.6	17.1	12.6
10065, 145	8.2	41.2	7.8	16.8	13.2
Highland soils					
60009, 621 Core, immature-submature	5.9	46.1	0.6	5.2	16.6
60009, 619 Core, immature-submature	5.9	46.1	0.6	5.2	16.6
60010, 1257 Core, submature-mature	5.9	46.1	0.6	5.2	16.6
60013, 319 Core, submature	NA	54.8	NA	NA	NA
60014, 197 Core, mature	NA	54.8	NA	NA	NA
61501, 120 submature	6.1	44.7	0.5	5.3	15.3
Mare soils					
12025, 351 Core	NA	NA	NA	NA	NA
12028, 83 Core	NA	NA	NA	NA	NA
70002, 461 Core, submature	10.1	42.3	5.8	15.4	11.2
70003, 537 Core, submature	10.0	42.6	5.7	15.3	11.0
70004, 574 Core, submature-mature	10.2	42.2	5.7	16.7	10.5
70005, 485 Core, mature	9.9	42.1	5.4	16.0	11.8
70007, 452 Core, submature	10.1	41.7	6.0	15.9	11.3
70008, 513 Core, immature	9.6	39.5	9.1	18.3	11.2
70009, 550 Core, submature	10.7	40.4	8.3	17.1	10.9

NA = not available. Major element data (wt.%) of lunar samples are from lunar sample compendium (Meyer, 2004–2011) and mare basalt database (Neal, 2008). The data for 61501 is from Morris (1978) and Morris et al. (1983). Breccia maturity data are from Korotev and Morris (1993), Meyer, 2004–2011 and Morris et al. (1979).

[a] Orang glass beads.

Table 2
Magnesium isotopic compositions of reference materials.

Samples	$\delta^{26}Mg$[a]	2SD[b]	$\delta^{25}Mg$[a]	2SD[b]
IL-lunar[c]	0.00	0.08	−0.02	0.06
	−0.07	0.05	−0.04	0.09
	−0.02	0.08	0.00	0.05
	−0.03	0.05	−0.03	0.03
	−0.01	0.07	−0.01	0.05
Average[d] ($n = 5$)	−0.03	0.03	−0.02	0.02
IL-granite[e]	−0.06	0.06	−0.02	0.03
	−0.05	0.06	−0.02	0.04
	0.01	0.07	−0.01	0.05
	−0.05	0.04	−0.05	0.03
	−0.01	0.05	−0.02	0.05
Average ($n = 5$)	−0.04	0.02	−0.03	0.02
KH-1 olivine[f]	−0.32	0.04	−0.16	0.04
	−0.29	0.03	−0.12	0.04
	−0.32	0.06	−0.13	0.03
	−0.28	0.06	−0.13	0.03
	−0.32	0.04	−0.16	0.04
	−0.33	0.05	−0.15	0.05
	−0.28	0.03	−0.12	0.07
	−0.28	0.06	−0.17	0.04
Average ($n = 8$)	−0.30	0.01	−0.14	0.01

[a] $\delta^{x}Mg = [(^{x}Mg/^{24}Mg)_{sample}/(^{x}Mg/^{24}Mg)_{DSM3} - 1] \times 1000$, where $x = 25$ or 26 and DSM3 is Mg solution made from pure Mg metal (Galy et al., 2003).

[b] 2SD = 2 times the standard deviation of the population of n ($n > 20$) repeat measurements of the standards during an analytical session.

[c] IL-lunar is a synthetic solution with Mg:Fe:Ca:Ti:Ni = 1:4:4:4:0.1.

[d] Average is weighted average calculated based on inverse-variance weighted model using Isoplot 3.75–4.15.

[e] IL-granite is a synthetic solution with Mg:Fe:Al:Ca:Na:K:Ti:Ni = 1:5:30:5:10:20:0.1:0.

[f] KH-1 olivine is an in-house standard that has been analyzed through whole-procedural column chemistry and instrumental analysis with $\delta^{26}Mg = -0.27 \pm 0.07$ (2SD) and $\delta^{25}Mg = -0.14 \pm 0.04$ (2SD) (Liu et al., 2010; Teng et al., 2010).

are subdivided into olivine, pigeonite, and ilmenite basalts (Neal and Taylor, 1992; Neal et al., 1994). The mare basalts from Apollo 15 are sub-classified into quartz- and olivine-normative basalts (Chappell and Green, 1973). High-Ti mare basalts have been classified into ten subgroups based on their mineralogy and trace-element characteristics (Neal and Taylor, 1992) (Tables 1 and 3).

Mare basalts investigated here include low-Ti basalts from Apollo 12 ($n = 6$, ranging from olivine, pigeonite to ilmenite basalts) and Apollo15 ($n = 6$, ranging from quartz-normative to olivine-normative basalts) and high-Ti basalts from Apollo 11 ($n = 2$, one B3 type olivine basalt (low K, low La) and one A type ilmenite basalt (high K, high La)) and Apollo17 ($n = 8$, ranging from low K, low La to high K and high La basalts) missions (Tables 1 and 3). In addition to these mare basalts, orange glass beads from Apollo 17, 74220, were also studied here. Relative to mare basalts, glass samples are more primitive and hence may provide more direct information on composition of the lunar mantle (Delano and Lindsley, 1983; Delano 1986; Shearer and Papike, 1993). Both mare basalts and volcanic glasses are referred as mare basalts in our later discussion.

2.3. Regolith breccias

Lunar breccias, produced by single or multiple impacts, are mixtures of mineral and rock fragments, crystallized impact melts, or glassy-impact melts. Polymict breccias are classified into glassy melt, crystalline melt, fragmental, clast-poor impact melt, granulitic, dimict, and regolith breccias (Stöffler et al., 1980). The lunar breccias studied here are Apollo 11 regolith breccias that consist mostly of high-Ti mare basalt components (e.g., Rhodes and Blanchard, 1982) (Table 1).

2.4. Lunar soils

Lunar soil is defined to be particles < 1 cm and blankets the surface of the Moon. It is formed and altered mainly by micrometeorite (<1 mm) bombardment, with minor modifications due to solar-wind and cosmic-rays particles (McKay et al., 1991). Composition of lunar soils ranges from basaltic to anorthositic with a small meteoritic component (<2 vol.%) (McKay et al., 1991). The samples studied here include six highland soils from Apollo 16 drill cores, two mare soils from an Apollo 12 drive tube, and seven mare soils from Apollo 17 drill cores (Meyer, 2004–2011) (Table 1). The sampling depth for these samples varies from 50 cm to 3 m with different degree of maturity and modal mineralogy, as well as chemical composition (Fryxell and Heiken, 1974; Meyer, 2004–2011).

3. ANALYTICAL METHODS

The Mg isotopic analyses were conducted at the Isotope Laboratory of the University of Arkansas at Fayetteville following a modified procedure after Yang et al. (2009), Li et al. (2010), and Teng et al. (2007, 2010).

3.1. Sample dissolution

Approximately 1–10 mg aliquots of each sample, based on the Mg concentration, were dissolved in a mixture of concentrated HF–HNO_3 (~3:1) (v/v), in Savillex screw-top beakers and heated overnight at a temperature of ~160 °C, on a hot plate in a fume hood. The sample solutions were then dried at 120 °C. To achieve 100% dissolution, the dried samples were dissolved in a mixture of HCl–HNO_3 (~3:1) (v/v) and heated at a temperature of 160 °C for 1–2 days. After evaporation of the solutions into dry substance, the samples were refluxed with concentrated HCl and then evaporated into dryness again. The dried residues were finally dissolved in a mixture of 1 N HCl–0.5 N HF, and no residue was observed in the solution.

3.2. Column chemistry and instrumental analysis

The column chemistry involves two steps. The first step was performed mainly to separate Ti from Mg by following

Table 3
Magnesium isotopic compositions of lunar samples.

Sample	$\delta^{26}Mg$[a]	2SD[b]	$\delta^{25}Mg$[a]	2SD[b]
Volcanic rocks:				
Mare basalts				
10020, 222 High-Ti basalt	−0.56	0.06	−0.28	0.04
Replicate[c]	−0.60	0.06	−0.30	0.03
Replicate	−0.54	0.06	−0.26	0.05
Replicate	−0.56	0.06	−0.31	0.05
Replicate	−0.58	0.08	−0.32	0.05
Replicate	−0.61	0.03	−0.31	0.05
Replicate-Ti[d]	−0.59	0.04	−0.30	0.06
Average[e]	−0.59	0.02	−0.30	0.02
10049, 89 High-Ti, High-K basalt	−0.39	0.09	−0.20	0.07
Replicate	−0.40	0.04	−0.20	0.04
Replicate	−0.33	0.05	−0.18	0.03
Replicate-Ti	−0.35	0.05	−0.14	0.04
Average	−0.37	0.02	−0.18	0.02
12002, 240 Low-Ti basalt	−0.28	0.06	−0.15	0.07
Duplicate[f]	−0.30	0.07	−0.13	0.04
Average	−0.29	0.05	−0.14	0.04
12005, 46 Low-Ti basalt	−0.24	0.04	−0.11	0.03
Replicate	−0.27	0.06	−0.14	0.07
Average	−0.25	0.03	−0.12	0.03
12051, 48	−0.27	0.06	−0.13	0.04
Replicate	−0.30	0.06	−0.17	0.03
Average	−0.28	0.04	−0.16	0.02
12011, 25 Low-Ti basalt	−0.22	0.07	−0.11	0.04
Duplicate	−0.23	0.08	−0.10	0.05
Replicate	−0.22	0.06	−0.17	0.10
Average	−0.22	0.04	−0.11	0.03
12021,574 Low-Ti basalt	−0.34	0.04	−0.16	0.04
Replicate	−0.34	0.06	−0.21	0.05
Replicate	−0.28	0.08	−0.16	0.08
Average	−0.33	0.03	−0.18	0.03
12052, 330 Low-Ti basalt	−0.20	0.06	−0.10	0.06
Duplicate	−0.18	0.08	−0.09	0.04
Average	−0.19	0.05	−0.09	0.04
15058, 239 Low-Ti basalt	−0.32	0.04	−0.16	0.04
15075, 52 Low-Ti basalt	−0.29	0.05	−0.14	0.05
Replicate	−0.23	0.06	−0.16	0.04
Average	−0.26	0.04	−0.15	0.03
15475, 187 Low-Ti basalt	−0.19	0.04	−0.12	0.03
Replicate	−0.22	0.08	−0.08	0.08
Replicate	−0.23	0.06	−0.14	0.04
Replicate	−0.22	0.03	−0.10	0.04
Average	−0.22	0.02	−0.12	0.02
15499, 13 Low-Ti basalt	−0.21	0.09	−0.12	0.05
15016, 221 Low-Ti basalt	−0.24	0.06	−0.09	0.03
Replicate	−0.20	0.06	−0.07	0.04
Average	−0.22	0.04	−0.09	0.02
15555 Low-Ti basalt	−0.01	0.05	0.01	0.03
Replicate	−0.04	0.06	−0.01	0.08
Replicate	−0.03	0.08	−0.05	0.08
Duplicate	0.02	0.06	0.01	0.04
Average	−0.02	0.03	0.00	0.02
70035, 9 High-Ti basalt	−0.53	0.05	−0.27	0.05
Replicate	−0.46	0.04	−0.22	0.03
Replicate	−0.40	0.09	−0.18	0.09
Replicate-Ti	−0.43	0.09	−0.24	0.07
Average	−0.47	0.07	−0.23	0.03

Table 3 (*continued*)

Sample	$\delta^{26}Mg$[a]	2SD[b]	$\delta^{25}Mg$[a]	2SD[b]
71539, 17 High-Ti basalt	−0.40	0.06	−0.19	0.04
Duplicate	−0.44	0.06	−0.24	0.04
Replicate-Ti	−0.45	0.03	−0.24	0.03
Average	−0.44	0.02	−0.23	0.02
75015, 1 High-Ti basalt	−0.53	0.05	−0.26	0.05
Replicate	−0.47	0.09	−0.25	0.09
Replicate-Ti	−0.48	0.06	−0.24	0.06
Average	−0.50	0.04	−0.25	0.04
70215, 322 High-Ti basalt	−0.51	0.05	−0.24	0.05
Duplicate	−0.50	0.06	−0.23	0.04
Average	−0.51	0.04	−0.24	0.03
75075, 171 High-Ti basalt	−0.40	0.06	−0.22	0.04
Replicate	−0.44	0.05	−0.25	0.05
Replicate	−0.40	0.09	−0.23	0.09
Duplicate	−0.42	0.06	−0.17	0.04
Replicate-Ti	−0.43	0.07	−0.23	0.02
Average	−0.42	0.03	−0.22	0.01
74255, 185 High-Ti basalt	−0.60	0.05	−0.27	0.05
Duplicate	−0.53	0.06	−0.26	0.04
Replicate-Ti	−0.50	0.08	−0.24	0.07
Replicate	−0.52	0.04	−0.25	0.05
Average	−0.54	0.07	−0.25	0.02
70017, 524 High-Ti basalt	−0.57	0.05	−0.27	0.05
Replicate	−0.51	0.04	−0.24	0.04
Average	−0.53	0.03	−0.25	0.03
Mare pyroclastic glasses				
74220, 758	−0.27	0.05	−0.14	0.05
Replicate	−0.34	0.04	−0.21	0.03
Average	−0.31	0.03	−0.19	0.03
Highland rocks				
14310, 631 Impact melt	−0.26	0.08	−0.12	0.04
Duplicate	−0.26	0.08	−0.12	0.05
Replicate	−0.29	0.04	−0.14	0.03
Average	−0.28	0.03	−0.13	0.03
60315, 30 Plagioclase clasts	−0.28	0.09	−0.13	0.05
Replicate	−0.34	0.04	−0.17	0.04
Average	−0.34	0.03	−0.16	0.03
68415, 200 Clast-poor impact melt	−0.18	0.06	−0.08	0.04
Regolith breccias				
10018, 101	−0.14	0.08	−0.09	0.06
Replicate	−0.22	0.05	−0.11	0.05
Average	−0.20	0.04	−0.10	0.04
10019, 85	−0.29	0.05	−0.17	0.05
Replicate	−0.27	0.04	−0.14	0.03
Replicate	−0.31	0.04	−0.16	0.03
Replicate	−0.27	0.09	−0.12	0.03
Average	−0.29	0.02	−0.14	0.02
10021, 90	−0.17	0.07	−0.08	0.06
10046, 231	−0.16	0.07	−0.10	0.06
10048, 198	−0.17	0.09	−0.08	0.07
10060, 136	−0.21	0.07	−0.11	0.06
10065, 145	−0.32	0.07	−0.16	0.05
Duplicate	−0.33	0.05	−0.16	0.03
Replicate	−0.28	0.04	−0.11	0.04
Replicate	−0.29	0.08	−0.13	0.05
Average	−0.30	0.03	−0.14	0.02
Highland soils				
60009, 621 Core, immature-submature	−0.18	0.06	−0.08	0.07
60009, 619 Core, immature-submature	−0.17	0.06	−0.08	0.07

(*continued on next page*)

Table 3 (*continued*)

Sample	$\delta^{26}Mg$[a]	2SD[b]	$\delta^{25}Mg$[a]	2SD[b]
Replicate	−0.22	0.05	−0.12	0.05
Average	−0.20	0.04	−0.11	0.04
60010, 1257 Core, submature-mature	−0.16	0.08	−0.10	0.06
Replicate	−0.22	0.05	−0.12	0.05
Average	−0.20	0.04	−0.11	0.04
60013, 319 Core, submature	−0.16	0.09	−0.08	0.07
Duplicate	−0.18	0.06	−0.09	0.07
Average	−0.17	0.05	−0.08	0.05
60014, 197 Core, mature	−0.14	0.07	−0.07	0.07
Duplicate	−0.19	0.09	−0.07	0.07
Average	−0.16	0.06	−0.07	0.05
61501, 120 Highland soil, submature	−0.23	0.05	−0.08	0.05
Duplicate	−0.19	0.07	−0.09	0.05
Replicate	−0.15	0.06	−0.08	0.03
Replicate	−0.20	0.04	−0.09	0.01
Average	−0.19	0.03	−0.09	0.01
Mare soils				
12025, 351 Core	−0.24	0.09	−0.12	0.07
Replicate	−0.24	0.05	−0.15	0.05
Replicate	−0.29	0.08	−0.15	0.05
Replicate	−0.28	0.06	−0.11	0.03
Average	−0.26	0.03	−0.12	0.02
12028, 835 Core	−0.25	0.07	−0.11	0.05
Replicate	−0.27	0.05	−0.12	0.05
Average	−0.27	0.04	−0.12	0.03
70002, 461 Core	−0.21	0.08	−0.11	0.05
70003, 537 Core	−0.20	0.09	−0.11	0.07
Duplicate	−0.26	0.06	−0.11	0.05
Average	−0.24	0.05	−0.11	0.04
70004, 574 Core, submature-mature	−0.21	0.08	−0.11	0.07
Replicate	−0.26	0.05	−0.13	0.05
Average	−0.24	0.04	−0.12	0.04
70005, 485 Core, mature	−0.33	0.07	−0.17	0.05
Replicate	−0.30	0.06	−0.14	0.03
Average	−0.31	0.05	−0.15	0.02
70007, 452 Core, submature	−0.26	0.08	−0.13	0.05
70008, 513 Core, immature	−0.36	0.04	−0.16	0.03
Replicate	−0.41	0.04	−0.19	0.04
Replicate	−0.41	0.05	−0.17	0.03
Replicate	−0.39	0.02	−0.19	0.03
Replicate-Ti	−0.38	0.05	−0.20	0.06
Average	−0.39	0.02	−0.18	0.02
70009, 550 Core, submature	−0.29	0.08	−0.13	0.07
Replicate	−0.33	0.06	−0.16	0.04
Replicate	−0.34	0.05	−0.18	0.05
Average	−0.33	0.04	−0.16	0.03

[a] $\delta^{x}Mg = [(^{x}Mg/^{24}Mg)_{sample}/(^{x}Mg/^{24}Mg)_{DSM3} - 1] \times 1000$, where $x = 25$ or 26 and DSM3 is Mg solution made from pure Mg metal (Galy et al., 2003).

[b] 2SD = 2 times the standard deviation of the population of n ($n > 20$) repeat measurements of the standards during an analytical session

[c] Replicate: Repeat the main-Mg column chemistry from the same stock sample solution.

[d] Replicate-Ti: Repeat Ti column chemistry after the main-Mg column chemistry and isotopic analyses.

[e] Average is weighted average calculated based on inverse-variance weighted model using Isoplot 3.75–4.15.

[f] Duplicate: Repeated measurement of Mg isotopic ratios on the same solution.

the method described in Cook et al. (2006). In brief, a small-volume (~2 ml) ion-exchange column packed with Bio-Rad 200–400 mesh AG1-X8 resin, pre-cleaned (rinsed 14 times column volume of 4 N HCl, 1 N HNO_3 and 18.2 MΩ Milli-Q® water) was used. The samples were loaded on the resin in 0.2 mL of 1 N HCl–0.5 N HF. The first 5 mL of 1 N HCl–0.5 N HF separated Mg from Ti. To assure the accuracy of our data, at least two reference materials, with comparable Mg:Ti ratios, were included in each batch of processed samples. To check the efficiency of Ti column chemistry, the Ti/Mg ratio in purified Mg sample solutions was measured and was <0.05. For most

high-Ti samples, the Ti column chemistry was repeated after the main-Mg column chemistry.

In the second step, the main-Mg column chemistry, with Bio-Rad 200–400 mesh AG50W-X8 resin in 1 N HNO_3 media, was used to separate Mg from other matrix elements, following previously established procedures (Teng et al., 2007, 2010; Yang et al., 2009; Li et al., 2010). Sample and reference solutions dissolved in 1 N HNO_3 (from the first step) were loaded on the resin and eluted through the column by 1 N HNO_3. Due to Mg isotope fractionation during ion exchange chromatography (Russell and Papanastassiou, 1978; Chang et al., 2003; Teng et al., 2007), the Mg cut was determined to assure 100% Mg yield with no elemental interferences (Teng et al., 2007, 2010; Li et al., 2010). Magnesium yields for all lunar and standard samples are >99%. The main-Mg column chemistry was repeated for all lunar samples and reference materials to ensure that the ratio of the concentration of any interfering cations to that of Mg is <0.05. Magnesium isotopic analyses were performed by the standard-bracketing method using a Nu Plasma MC-ICPMS. The concentrations of the sample solution and standard were matched within 10% to avoid the matrix effect caused by concentration mismatch. The purified Mg sample solution (~250–300 ppb Mg in ~3% (v/v) or ~0.45 N HNO_3 solution) was introduced into a "wet" plasma and Mg isotopes were analyzed in a low-resolution mode, with ^{26}Mg, ^{25}Mg, and ^{24}Mg measured simultaneously, in separate Faraday cups (H5, Ax, and L4).

3.3. Precision and accuracy

Long-term external precision and accuracy of Mg isotopic analyses at the Isotope Laboratory of the University of Arkansas were evaluated by full-procedural replicate analyses of seawater, rocks, minerals, synthetic solutions, and pure Mg Cambridge-1 standard solution (Teng et al., 2010; Li et al., 2010; Ling et al., 2011). The in-run precision on the $^{26}Mg/^{24}Mg$ ratio for a single measurement of one block of 40 ratios was $< \pm 0.02‰$ (2SD). The long-term external precisions for $\delta^{26}Mg$ and $\delta^{25}Mg$ are better than $\pm 0.07‰$ and $\pm 0.06‰$ (2SD), respectively (Li et al., 2010; Teng et al., 2010; Ling et al., 2011).

In order to evaluate the precision and accuracy of Mg isotope data during the course of this study, full procedural replicate analyses were performed on two synthetic solutions (IL-granite and IL-lunar) and one in-house standard (Kilbourne Hole (KH-1) olivine) (Table 2). IL-granite and IL-lunar yielded weighted average $\delta^{26}Mg$ values of $-0.04 \pm 0.02‰$ ($n = 5$, Table 2) and $-0.03 \pm 0.03‰$ ($n = 5$, Table 2) respectively, which are identical to the expected value of 0 within uncertainty. The olivine KH-1 yielded a weighted average $\delta^{26}Mg$ value of $-0.30 \pm 0.01‰$ ($n = 8$, Table 2), which agrees with the values reported by Teng et al. (2010) and Liu et al. (2010b) ($\delta^{26}Mg = -0.27 \pm 0.07‰$; 2SD, $n = 16$). The results of these synthetic and natural standard solutions confirm the accuracy and reproducibility of our measurements during this course of analyses. In addition, full procedural replicate analyses of samples and samples processed through additional Ti-column chemistry yielded identical $\delta^{26}Mg$ values (Table 3), further assuring the precision and reproducibility of our data.

4. RESULTS

Magnesium isotopic compositions are reported in Table 2 for reference samples and in Table 3 for lunar samples. All samples analyzed here, in addition to those of the bulk Earth, chondrites, and seawater reported by Teng et al. (2010) and Ling et al. (2011) from the same lab, fall on a single mass-dependent fractionation line with a best-fit slope of 0.505 (Fig. 2), which is consistent with previous studies (e.g., Young and Galy, 2004; Li et al., 2010; Teng et al., 2010). $\delta^{26}Mg$ values range from $-0.61 \pm 0.03‰$ to $0.02 \pm 0.06‰$ in mare basalts, from $0.34 \pm 0.04‰$ to $-0.18 \pm 0.06‰$ in highland rocks, from $-0.33 \pm 0.05‰$ to $-0.14 \pm 0.08‰$ in regolith breccias, from $-0.23 \pm 0.05‰$ to $-0.14 \pm 0.07‰$ in highland soil, and from $-0.41 \pm 0.05‰$ to $-0.20 \pm 0.09‰$ in mare soil samples (Fig. 3). The range of Mg isotopic variation in lunar basalts (~0.628‰ for $\delta^{26}Mg$) is significantly larger than the analytical uncertainty (Table 3 and Fig. 3).

Generally, $\delta^{26}Mg$ values display a dichotomy between low-Ti and high-Ti basalts. All low-Ti basalts, except for sample 15555, are similar in Mg isotopic compositions, with an average $\delta^{26}Mg$ value of $-0.25 \pm 0.10‰$. By contrast, high-Ti basalts display a larger variation, with an average $\delta^{26}Mg$ value of $-0.49 \pm 0.14‰$. Basalt sample 15555 has the highest $\delta^{26}Mg$ value among all lunar samples ($-0.02 \pm 0.03‰$, 2SD, $n = 4$). Different aliquots of this sample also display distinct $\delta^{18}O$ values (5.443–5.769‰) (Spicuzza et al., 2007; Liu et al., 2010a). This sample also displays large chemical variations among different chips, which may be attributed to a biased sampling owing to the large grain size (e.g., Ryder and Schuraytz, 2001). Therefore, the heavy Mg isotopic composition of sample

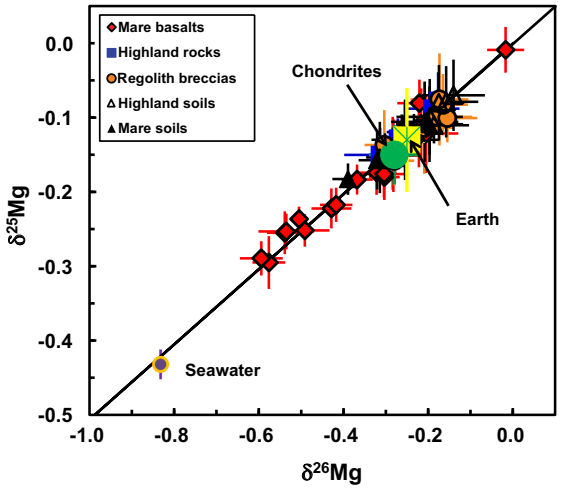

Fig. 2. Magnesium three-isotope plot of lunar samples analyzed in this study. Compositions of the Earth and chondrites (Teng et al., 2010) as well as seawater (Ling et al., 2011) are also plotted for comparison. The solid line represents a mass-dependent fractionation line with a slop of 0.505. Data are reported in Table 3.

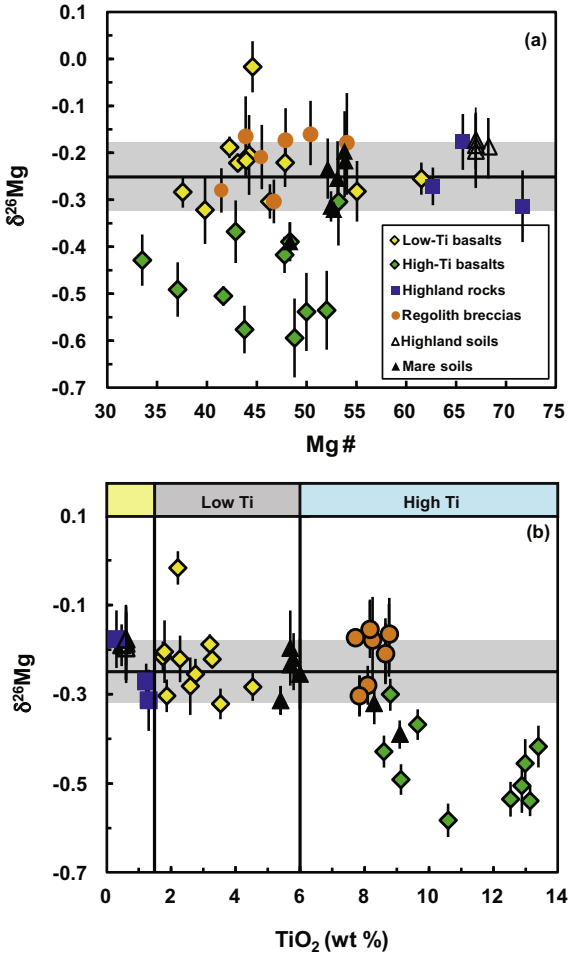

Fig. 3. Variation of δ^{26}Mg versus MgO (a) and TiO_2 (b) contents in lunar samples studied here. The solid line and grey bar represent the average δ^{26}Mg of −0.25‰ and two standard deviation of ±0.07‰ for the Earth (Teng et al., 2010). Data are reported in Tables 1 and 3.

15555 may have resulted from the heterogeneous mineral distribution in this sample. Future studies are needed to better understand the mechanisms of producing heavy Mg isotopic composition.

Compared to previous studies of limited lunar samples, our Mg data are systematically lighter than those of Wiechert and Halliday (2007), but are heavier than those of Chakrabarti and Jacobsen (2010). The difference between low-Ti and high-Ti basalts analyzed here is similar to the variation reported by Wiechert and Halliday (2007), but different from Chakrabarti and Jacobsen (2010). Differences among these groups are likely the result of inter-laboratory biases, which makes it impractical to conduct cross-comparison among different datasets. However, given the reproducibility for each lab, the range of variation in lunar samples is a meaningful comparison.

5. DISCUSSION

The Moon is thought to have been partially molten to depths of 400–500 km (Pritchard and Stevenson, 2000; Canup, 2004) after the giant impact that formed the Moon (Hartmann and Davis, 1975; Cameron and Ward, 1976). Fractional crystallization of this magma ocean (LMO) led to the formation of a feldspathic crust and a mafic mantle (Warren, 1985). A highly fractionated, late-stage liquid with significant amounts of ilmenite also crystallized at the end of the LMO solidification between the deep mafic cumulates and the anorthositic crust (Warren, 1985; Shearer and Papike, 1999). This last portion of the highly differentiated LMO, termed urKREEP, crystallized beneath the anorthositic crust (Warren, 1985).

In this section, we first discuss the behavior of Mg isotopes during lunar soil formation and lunar magmatic differentiation. Then, we estimate the average Mg isotopic composition of the Moon and finally evaluate the extent of Mg isotopic heterogeneity in the early solar system.

5.1. Magnesium isotopic systematics of lunar soils and regolith breccias

Lunar soils and regolith breccias are mixtures of diverse rock types and components, hence may be more representative of the average composition of the Moon than individual crystalline rocks. Previous studies have found large grain surface-correlated mass-dependent kinetic isotope fractionation effects e.g., for O, S, Si, K, Ca, Mg and Fe (e.g., Epstein and Taylor, 1971; Clayton et al., 1974; Russell et al., 1977; Esat and Taylor, 1992; Humayun and Clayton, 1995a; Wiesli et al., 2003). These isotope fractionation effects were sample surface correlated and not representative of the bulk samples. They were interpreted as results of ion sputtering by the solar wind and galactic cosmic rays, and/or vaporization by micrometeorite impacts followed by gravitational mass selection (loss of the lighter isotopes) and re-deposition of the heavier isotopes (e.g., Switkowski et al., 1977; Housley, 1979).

The lunar soils and regolith breccias analyzed in this study, except for one sample, have similar Mg isotopic compositions to the Earth, despite the difference in their bulk-rock compositions (Figs. 2 and 3). This conclusion is similar to previous studies of bulk soils (Esat and Taylor, 1992; Chakrabarti and Jacobsen, 2011), suggesting that irradiation or micrometeorite impacts does not affect Mg isotopic compositions of bulk samples. Hence, these samples can be used to estimate the average Mg isotopic composition of the Moon (see details in Section 5.3).

5.2. Magnesium isotopic systematics of lunar basalts

The lunar basalts studied here have variable Mg isotopic compositions. The low-Ti basalts with <6 wt.% TiO_2 have similar δ^{26}Mg to those of highland rocks, regolith breccias, and mare and highland soils. By contrast, all high-Ti basalts (except for one) are light in Mg isotopic compositions (Fig. 3). This trend is similar to the one observed in Wiechert and Halliday (2007), despite the inter-laboratory bias. The dichotomy between low- and high-Ti basalts has been reported in stable isotopes of O, Li, and Fe (Magna et al., 2006; Seitz et al., 2006; Spicuzza et al., 2007; Craddock et al., 2010; Hallis et al., 2010; Liu et al., 2010a). These

differences were suggested to be due to heterogeneous mantle sources for low- and high-Ti basalts, which are also consistent with petrological, mineralogical, geochemical, and radiogenic isotopic studies of these basalts (e.g., Neal and Taylor, 1992; Snyder et al., 1992; Beard et al., 1998; Shearer et al., 2006; Brandon et al., 2009).

Below, we first determine the major mineral phases that control MgO budget and then discuss the potential factors that control Mg isotopic variation in both low-Ti and high-Ti basalts.

5.2.1. Magnesium concentration variations in lunar basalts

For Mg-bearing minerals, clinopyroxene is the most abundant phase, followed by opaques including ilmenite, chromian ulvöspinel and armalcolite in the high-Ti basalts, while olivine and low-Ca pyroxene dominate the low-Ti basalts. Mineral abundances versus MgO plots reveal no significant correlation between pyroxene (41–71 vol.%) and MgO (Fig. 4b). However, there is clear positive correlation between olivine (0–30 vol.%) and MgO contents in low-Ti basalts, and a positive correlation between opaque minerals (15–25 vol.%) and MgO contents in high-Ti basalts (Fig. 4a and c). These positive correlations indicate that olivine controls the MgO variation in low-Ti basalts whereas opaque minerals play a key role in controlling the MgO variation in high-Ti basalts, with a buffering role of pyroxene in both basalt types.

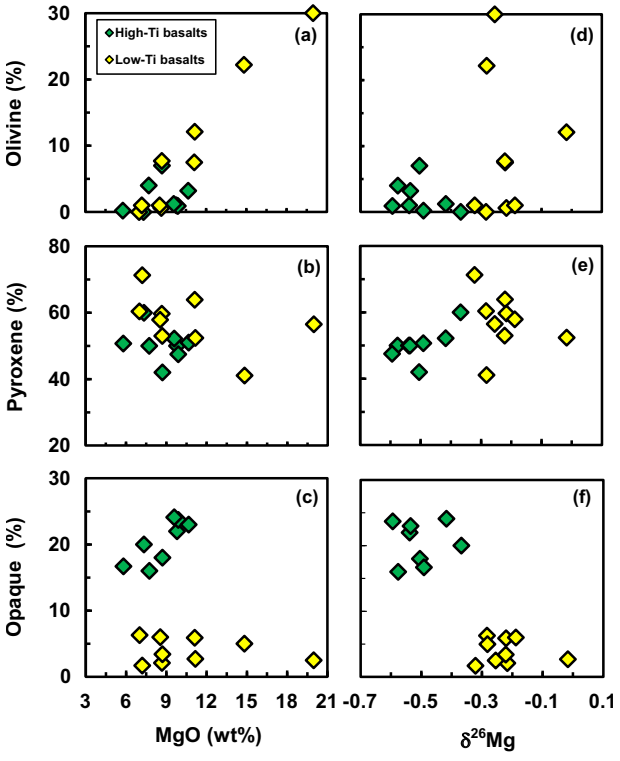

Fig. 4. Olivine, pyroxene, and opaque modal abundances (%) vs. MgO (wt.%) (a–c) and δ^{26}Mg (‰) (d–f) of the whole rock samples of lunar basalts investigated in this study. Mineral abundances for lunar samples are from lunar sample compendia (Meyer, 2004–2011).

Ilmenite [(Fe, Mg)TiO_3], armalcolite [$(Mg_{0.5}{\cdot}Fe_{0.5})Ti_2O_5$], and chromian ulvöspinel [$(Mg, Fe)(Al, Cr)_2O_4$] are the Fe–Ti oxides containing Mg in lunar basalts. Armalcolite and chromian ulvöspinel can contain significant amount of MgO but they should not significantly affect the MgO budget of high-Ti basalts because of their low modal abundance (<0.5 wt.%, Warner et al., 1978). By contrast, the modal abundance of ilmenite in high-Ti basalts can be up to 28% (Papike et al., 1998). This, together with their high MgO content (3–8 wt.% e.g., Papike et al., 1998; Lucey et al., 2006; Van Kan Parker et al., 2011), may effectively be sufficient enough to affect the MgO contents of bulk basalts (e.g., Papike et al., 1998). Comparison of chemical compositions of low-Ti and high-Ti basalts supports the above conclusion. Both CaO and SiO_2 contents in low-Ti and high-Ti basalts decrease with MgO for samples investigated in this study and literature, reflecting crystallization of different mineral phases e.g., olivine, pyroxene and plagioclase (Fig. 5a and b). However, at a given MgO value, high-Ti basalts always have lower SiO_2 contents than low-Ti basalts (Fig. 5b), indicating the presence of an additional phase that is enriched in MgO but depleted in SiO_2 in high-Ti basalts. On the other hand, TiO_2 positively correlates with MgO in high-Ti basalts and displays no correlation with MgO in low-Ti basalts (Fig. 5c). If ilmenite contained little MgO, a negative correlation between TiO_2 and MgO would be expected because of the dilution effect. These correlations thus further suggest that opaque minerals (i.e., ilmenite) not only control TiO_2 contents but also play a key role in MgO variations of high-Ti basalts.

5.2.2. Origins of light Mg isotopic composition of high-Ti basalts

The mantle sources for low-Ti and high-Ti basalts were cumulates formed in LMO, with the high-Ti basalts from late-stage ilmenite-rich cumulates. The O and Fe isotopic compositions of mare basalts have consistently revealed that the ilmenite crystallized in the LMO may be the cause for the observed differences (Craddock et al., 2010; Liu et al., 2010a). Our data here also indicate that ilmenite has a light Mg isotopic composition. δ^{26}Mg of lunar basalts does not correlate with $Mg^{\#}$ (index of crystallization) (Fig. 3a), or modal abundances of olivine and pyroxene (Fig. 4d and e), suggesting that crystallization of olivine and pyroxene did not significantly fractionate Mg isotopes. Instead, Mg isotopic compositions of lunar basalts decrease with TiO_2 and display a dichotomy between low- and high-Ti basalts (Fig. 3b). In addition, low- and high-Ti basalts display two clusters with high-Ti basalts enriched in opaque minerals and light Mg isotopes (Fig. 4f). These suggest that opaque minerals (i.e., ilmenite) have light Mg isotopic compositions and shift high-Ti basalts to lower δ^{26}Mg values.

The isotopically light ilmenite may result from equilibrium isotope fractionation in LMO. Studies of natural minerals and theoretical calculation have found large equilibrium inter-mineral Mg isotope fractionation (Handler et al., 2009; Yang et al., 2009; Young et al., 2009; Liu et al., 2010b, 2011; Schauble, 2011; Li et al., 2011; Wang et al., 2012; Xiao et al., 2013). This fractionation is qualitatively related to the different coordination number

(CN) of Mg bonded to O in minerals, as lower CN results in stronger bonds and favors heavy isotopes (e.g., Urey, 1947; Chacko et al., 2001). The CN of Mg in ilmenite is 6 (Raymond and Wenk, 1971; Lind and Housley, 1972), identical to that in olivine and pyroxene. Nonetheless, Schauble (2011) shows that significant Mg isotope fractionation occurs among different mineral species from carbonates, silicates, to periclase groups, with carbonates lighter and periclase heavier than silicates, although CN of Mg in all these mineral groups is 6. Hence, ilmenite as an oxide mineral could be fractionated from olivine and pyroxene.

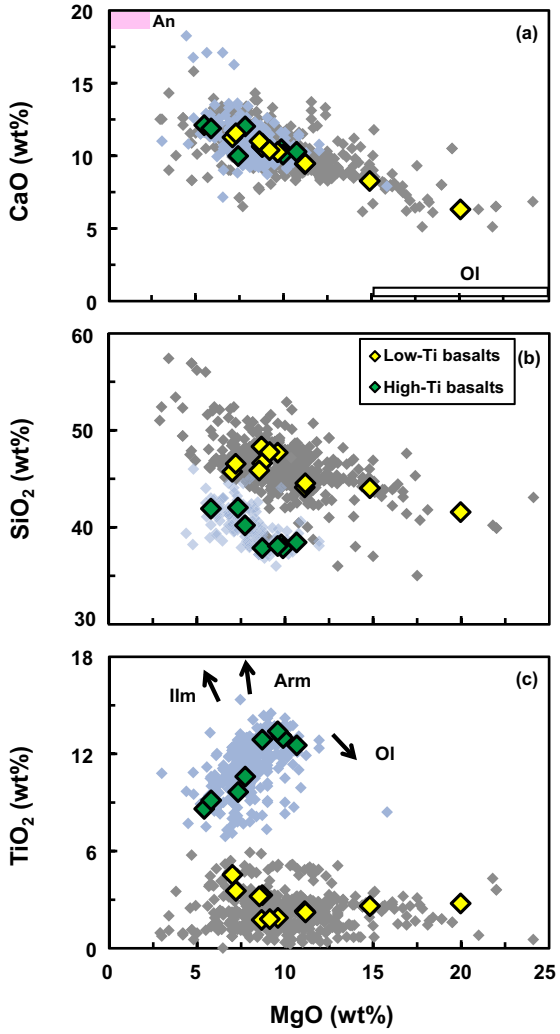

Fig. 5. CaO, SiO_2 and TiO_2 (wt.%) vs. MgO (wt.%) in lunar basalts investigated in this study. Grey and light blue diamonds represent low- and high-Ti basalts from mare basalt database (Neal, 2008), respectively. The large pink square on the top left corner on panel (a) represents the anorthosite samples ($\geqslant$90% plagioclase) with the lowest MgO. The rectangular on the lower right corner on the panel (a) represents the compositions of olivines from low- and high-Ti basalts (Papike et al., 1998). Arrows on panel (c) indicate the accumulation lines for armalcolite (Arm), ilmenite (Ilm), and olivine (Ol) (Papike et al., 1998). Data are from lunar sample compendia (Meyer, 2004–2011) and mare basalt database (Neal, 2008).

Alternatively, the light Mg isotopic composition of ilmenite versus olivine and pyroxene may result from diffusion-driven kinetic isotope fractionation in the LMO. Recent studies have shown that kinetic Mg and Fe isotope fractionations can occur during chemical and thermal diffusion in melts and between melts and minerals (Richter et al., 2008, 2009a,b; Huang et al., 2009; Teng et al., 2011). Coupled studies of Mg and Fe isotopes can tell chemical diffusion from thermal diffusion as a positive correlation between Mg and Fe isotope fractionations is expected for thermal diffusion and a negative correlation is for chemical diffusion. Since no δ^{26}Mg data are available for ilmenite, comparison of δ^{26}Mg and δ^{56}Fe data for lunar basalts is used here. Plots of δ^{26}Mg and δ^{56}Fe with TiO_2 display opposite trends and indicate a negative correlation between δ^{26}Mg and δ^{56}Fe in low- and high-Ti basalts (Fig. 6). Although the negative correlation may indicate that chemical diffusion can play a role in controlling Mg and Fe isotopic compositions of lunar basalts, petrological studies show that ilmenite in high-Ti basalts is one of the early crystallized phases, being in equilibrium with the melt and pyroxene, and it has probably not undergone post-magmatic re-equilibration (e.g., Warner et al., 1978; Shearer et al., 2006).

Although it is beyond the scope of this study, measurements of Mg isotopic compositions of ilmenite and other coexisting silicates in low- and high-Ti basalts need to be

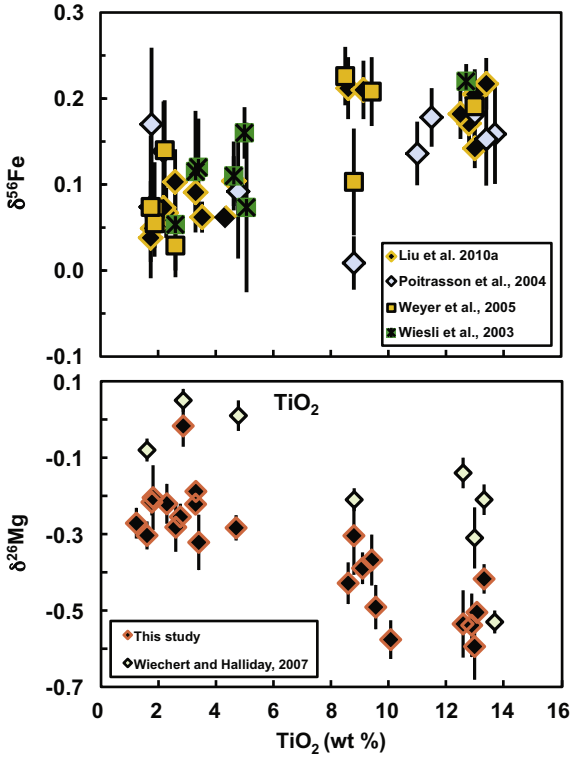

Fig. 6. δ^{56}Fe (Wiesli et al., 2003; Poitrasson et al., 2004; Weyer et al., 2005; Liu et al., 2010a) and δ^{26}Mg of lunar basalts (this study, Table 3; Wiechert and Halliday, 2007) versus their whole rock TiO_2 contents.

undertaken to solve the issue of whether Mg in lunar ilmenite is significantly fractionated from other minerals and the underlying mechanisms.

5.3. Magnesium isotopic composition of the Moon

Our knowledge on the structure and composition of the Moon comes from samples returned from Apollo and Luna missions, lunar meteorites, and remote sensing and seismic data (e.g., Taylor, 1982; Gillis et al., 2004; Weber et al., 2011). Based on these data, the Moon is believed to be differentiated with a feldspathic crust, a mafic mantle, and a partially molten core. The upper crust is more feldspathic with more gabbro and anorthositic gabbro and the lower crust is more mafic with more norite and anorthositic norite (Wieczorek et al., 2006). The upper mantle is enriched in pyroxene while the lower mantle is enriched in Mg-rich olivine (e.g., Warren, 1985; Shearer and Papike, 1999). The lunar crustal composition can be estimated by analysis of lunar samples such as ferroan anorthositic, magnesium and alkali suites, etc., as well as remote sensing data (e.g., Jolliff et al., 2000; Greenhagen et al., 2010; Chauhan et al., 2012). Unlike crust samples, no sample of lunar mantle has been discovered to date. The composition of the lunar mantle has been mainly studied through the analysis of partial melts of the lunar mantle, i.e., lunar basalts and volcanic glasses (Wieczorek et al., 2006). This method may not give an accurate estimate of the mantle source composition because of elemental and isotopic fractionation during the initial crystallization of the LMO. Pyroclastic glasses, with higher Mg, Ni, and $Mg^{\#}$, compared to the lunar basalts, are suggested to better constrain the lunar mantle composition because they represent the least differentiated melts (Delano and Lindsley, 1983; Delano, 1986; Shearer and Papike, 1993).

To date, four approaches have been utilized to estimate the isotopic composition of the bulk Moon: (1) the arithmetic mean of different types of lunar samples (e.g., Poitrasson et al., 2004); (2) the mean of the most primitive lunar samples, like green picritic glass 15426 (Wiechert and Halliday, 2007) or less fractionated material like orange glass 74220 and quartz-normative basalts (15058 and 15475) (Magna et al., 2006); (3) the mean of lunar samples excluding anomalies (e.g., Weyer et al., 2005); or 4) the mean of different sample weighted by their volumetric proportions (Liu et al., 2010a). Since different samples contribute to different volumetric proportions of the Moon, the arithmetic mean of these samples may not provide a precise estimate of the bulk isotopic composition of the Moon. In this study, we first estimate the Mg isotopic compositions of the lunar crust and mantle separately; then estimate the average composition of the bulk Moon, based on the weight percentage of the lunar crust and mantle.

Because of the limited Mg isotope fractionation during their formation processes, lunar highland impact-melt rocks and highland soil samples from Apollo 16 are used to estimate the lunar crust composition. The MgO-weighted average δ^{26}Mg value ($-0.24 \pm 0.07‰$) of these samples (14310, 60315, 68415, 60009, 60010, and 61501) is considered as the average Mg isotopic composition of the lunar crust. Since MgO contents of samples 60013 and 60014 are not available, these samples are not included in the calculation. All regolith breccias analyzed in this study are from mare regions, which are dominantly basaltic in bulk composition. Hence, these breccias, high-Ti basalts, and two mare soil samples (70008 and 70009) with >6 wt.% TiO_2 are used to estimate the MgO-weighted average δ^{26}Mg value of high-Ti basalts. The other mare soil samples from Apollo 17 with low TiO_2 contents are added to low-Ti basalts to estimate their MgO-weighted average δ^{26}Mg value. MgO contents of lunar soil 12025 and 12028 are not available; hence, these samples are not used to estimate the MgO-weighted average δ^{26}Mg value of low-Ti basalts. These average δ^{26}Mg values of low-Ti (excluding 15555) ($-0.25 \pm 0.05‰$) and high-Ti ($-0.36 \pm 0.14‰$) basalts are then used to estimate Mg isotopic composition of their mantle sources. Based on the Clementine remote sensing data for the lunar surface, low-Ti basalts are 90% of all mare basalts exposed on the lunar surface (Giguere et al., 2000). Using this estimated proportion and the average values of low- and high-Ti mantle sources, the weighted average δ^{26}Mg of the lunar mantle is estimated to be $-0.26 \pm 0.15‰$. By combining Mg isotopic compositions of the lunar crust and mantle and their weight percentage (7% and 93%, respectively; Warren, 2005), we estimate the weighted average δ^{26}Mg value of the bulk Moon to be $-0.26 \pm 0.16‰$. This value is considered as the best estimate of the average Mg isotopic composition of the Moon.

5.4. Chondritic Mg isotopic composition of the Moon and Earth

Studies of isotopic compositions of the Moon, Earth and chondrites can help to better understand the solar nebula conditions, proto-planetary disc processes, and the origin and evolution of the Earth–Moon system (e.g., Wiechert et al., 2001; Poitrasson et al., 2004; Wiechert and Halliday, 2007; Paniello et al., 2012). While it is well established now that the Earth has a chondritic Mg isotopic composition (Teng et al., 2007, 2010; Handler et al., 2009; Yang et al., 2009; Bourdon et al., 2010; Chakrabarti and Jacobsen, 2010; Dauphas et al., 2010; Schiller et al., 2010; Huang et al., 2011; Liu et al., 2011; Pogge von Strandmann et al., 2011; Xiao et al., 2013), there is still uncertainty on the Mg isotopic composition of the Moon because of the limited data (Warren et al., 2005; Norman et al., 2006; Wiechert and Halliday, 2007; Chakrabarti and Jacobsen, 2010). The wide range of lunar samples measured in this study, and those of terrestrial and chondritic samples analyzed in the same laboratory (Yang et al., 2009; Teng et al., 2010; Liu et al., 2011; Xiao et al., 2013), allows an internally-consistent comparison of Mg isotopic compositions among different planetary materials.

The Mg isotopic composition of the Moon ($\delta^{26}Mg = -0.26 \pm 0.16‰$) estimated here is indistinguishable from that of the Earth ($\delta^{26}Mg = -0.25 \pm 0.07‰$; 2SD, $n = 139$) and chondrites ($\delta^{26}Mg = -0.28 \pm 0.06‰$; 2SD, $n = 38$) measured in the same laboratory (Teng et al., 2010) (Fig. 7). Hence, our study suggests that the Moon and the Earth have chondritic Mg isotopic compositions,

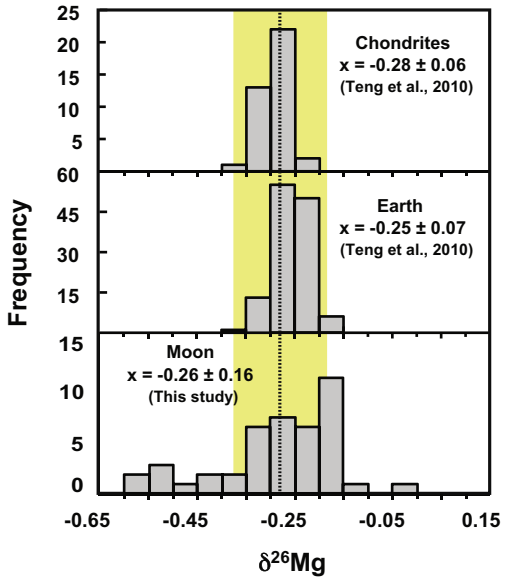

Fig. 7. Histogram of Mg isotopic compositions of the Moon, Earth and chondrites. The vertical dashed line and yellow bar represent the average δ^{26}Mg of −0.28‰ and two standard deviation of ±0.06‰ for chondrites (Teng et al., 2010).

reflecting extensive early disk mixing processes and homogeneity of Mg isotopes in the solar system. The chondritic Mg isotopic compositions of the Moon and the Earth also indicate that the Moon-forming giant impact did not fractionate Mg isotopes, in contrast from the models proposed for Fe isotopes (Poitrasson et al., 2004), but consistent with the lack of Li and K isotope fractionations in the Earth–Moon system (Humayun and Clayton, 1995b; Magna et al., 2006).

6. CONCLUSIONS

This study presents comprehensive Mg isotopic data for lunar samples including most types of available samples to date. The main conclusions are:

(1) δ^{26}Mg values range from -0.61 ± 0.03‰ to 0.02 ± 0.06‰ in mare basalts, from 0.34 ± 0.04‰ to -0.18 ± 0.06‰ in highland rocks, from -0.33 ± 0.05‰ to -0.14 ± 0.08‰ in regolith breccias, from -0.23 ± 0.05‰ to -0.14 ± 0.07‰ in highland soils, and from -0.41 ± 0.05‰ to -0.20 ± 0.09‰ in mare soil samples.

(2) The bulk mare and highland soils and regolith breccias have similar Mg isotopic compositions to those of the highland rocks, low-Ti basalts and the Earth, which indicates that their formation processes did not significantly fractionate Mg isotopes.

(3) High-Ti basalts are on average isotopically lighter than low-Ti basalts, mostly reflecting their heterogeneous cumulate sources produced during the lunar magmatic differentiation. The chemical and isotopic studies suggest that high abundance of ilmenite with possible lighter Mg isotopic composition than coexisting olivine and pyroxene may cause the light Mg isotopic composition of high-Ti basalts.

(4) Using the average Mg isotopic compositions of the lunar crust and mantle and their volumetric proportions, the weighted average Mg isotopic composition of the Moon is estimated to be -0.26 ± 0.16‰ for δ^{26}Mg and -0.13 ± 0.07‰ for δ^{25}Mg.

(5) The Moon (δ^{26}Mg $= -0.26 \pm 0.16$‰) has indistinguishable Mg isotopic composition from the Earth (δ^{26}Mg $= -0.25 \pm 0.07$‰) and chondrites (δ^{26}Mg $= -0.28 \pm 0.06$‰), suggesting the homogeneity of Mg isotopes in the solar system and the negligible Mg isotope fractionation during the Moon-forming giant impact.

ACKNOWLEDGEMENTS

We are grateful to Wang-Ye Li, Shan Ke and Sheng-Ao Liu for help in the lab, Kang-Jun Huang for discussion, and Walter Graupner for his help in maintaining the ICP-MS. The constructive comments from Dimitri Papanastassiou, Paul Tomascak and an anonymous reviewer significantly improved the manuscript. We also thank Dimitri Papanastassiou for the discussion and editorial handling of this manuscript. This work is supported by the National Science Foundation (EAR-0838227, EAR-1056713 and EAR-1340160) to FZT and NASA Cosmochemistry grant (NNX11AG58G) to LAT. YL participated the revision of this paper at Jet Propulsion Laboratory, which is managed by Caltech under the contract with NASA.

REFERENCES

Batchelor J. D., Symes S. J. K., Benoit P. H. and Sears D. W. G. (1997) Constraints on the thermal and mixing history of lunar surface materials and compositions with basaltic meteorites. *J. Geophys. Res.* **102**, 19321–19334.

Beard B. L., Taylor L. A., Scherer E. E., Johnson C. M. and Snyder G. A. (1998) The source region and melting mineralogy of high-titanium and low-titanium basalts deduced from Lu-Hf isotope data. *Geochim. Cosmochim. Acta* **62**, 525–544.

Bourdon B., Tipper E. T., Fitoussi C. and Stracke A. (2010) Chondritic Mg isotope composition of the Earth. *Geochim. Cosmochim. Acta* **74**, 5069–5083.

Brandon A. D., Lapen T. J., Debaille V., Beard B. L., Rankenburg K. and Neal C. (2009) Re-evaluating ^{142}Nd/^{144}Nd in lunar mare basalts with implications for the early evolution and bulk Sm/Nd of the Moon. *Geochim. Cosmochim. Acta* **73**, 6421–6445.

Cameron A. G. W. and Ward W. R. (1976) The origin of the Moon. *Proc. 7th Lunar Sci. Conf.* 120–122.

Canup R. M. (2004) Dynamics of lunar formation. *Annu. Rev. Astron. Astrophys.* **42**, 441–475.

Chacko T., Cole D. R. and Horita J. (2001) Equilibrium oxygen, hydrogen and carbon isotope fractionation factors applicable to geological systems. *Rev. Mineral. Geochem.* **43**, 1–82.

Chakrabarti R. and Jacobsen S. B. (2010) The isotopic composition of magnesium in the inner solar system. *Earth Planet. Sci. Lett.* **293**, 349–358.

Chakrabarti R. and Jacobsen S. B. (2011) The isotopic composition of magnesium in bulk lunar soils. *Lunar Planet. Sci. XLII*. Lunar Planet. Inst., Houston. #2006 (abstr.).

Chang V. T.-C., Makishima A., Belshaw N. S. and O'Nions R. K. (2003) Purification of Mg from low-Mg biogenic carbonates for isotope ratio determination using multiple collector ICP-MS. *J. Anal. At. Spectrom.* **18**, 296–301.

Chappell B. W. and Green D. H. (1973) Chemical compositions and petrogenetic relationships in Apollo 15 mare basalts. *Earth Planet. Sci. Lett.* **18**, 237–246.

Chauhan P., Kaur P., Srivastava N., Bhattacharya S., Ajai, Kiran Kumar A. S. and Goswami J. N. (2012) Compositional and morphological analysis of high resolution remote sensing data over central peak of Tycho crater on the Moon: Implication for understanding lunar interior. *Curr. Sci.* **102**, 1041–1046.

Clayton R. N. and Mayeda T. K. (1977) Correlated oxygen and magnesium isotope anomalies in Allende inclusions: I. Oxygen. *Geophys. Res. Lett.* **4**, 295–298.

Clayton R. N., Hurd J. M. and Mayeda T. K. (1973) Oxygen isotopic compositions of Apollo 15, 16, and 17 samples, and their bearing on lunar origin and petrogenesis. *Proc. 4th Lunar Sci. Conf*. 1535–1542.

Clayton R. N., Mayeda T. K. and Hurd J. M. (1974) Loss of oxygen, silicon, sulfur, and potassium from the lunar regolith. *Proc. 5th Lunar Sci. Conf*. 1801–1809.

Clayton R. N., Hinton R. W. and Davis A. M. (1988) Isotopic variations in the rock forming elements in meteorites. *Philos. Trans. R. Soc. London A* **325**, 483–501.

Cook D. L., Wadhwa M., Janney P. E., Dauphas N., Clayton R. N. and Davis A. M. (2006) High precision measurements of non-mass-dependent effects in nickel isotopes in meteoritic metal via multicollector ICPMS. *Anal. Chem.* **78**, 8477–8484.

Craddock P. R., Dauphas N. and Clayton R. N. (2010) Mineralogical control on iron isotopic fractionation during lunar differentiation and magmatism. *Lunar Planet. Sci. XXXXI*. Lunar Planet. Inst., Houston. #1230 (abstr.).

Dauphas N., Teng F.-Z. and Arndt N. T. (2010) Magnesium and iron isotopes in 2.7 Ga Alexo komatiites: Mantle signatures, no evidence for Soret diffusion, and identification of diffusive transport in zoned olivine. *Geochim. Cosmochim. Acta* **74**, 3274–3291.

Davis A. M., Hashimoto A., Clayton R. N. and Mayeda T. K. (1990) Isotope mass fractionation during evaporation of Mg_2SiO_4. *Nature* **347**, 655–658.

Delano J. W. (1986) Pristine lunar glasses: Criteria, data, and implications. *J. Geophys. Res.* **91**, D201–D213.

Delano J. and Lindsley D. (1983) Mare glasses from Apollo 17: Constraints on the Moon's bulk composition. *J. Geophys. Rev.* **88**, B3–B16.

Epstein S. and Taylor H. P. (1971) O18/O16, Si30/Si28, D/H and C13/C12 ratios in lunar samples. *Proc. 2nd Lunar Sci. Conf*. 1421–1441.

Esat T. M. and Taylor S. R. (1992) Magnesium isotope fractionation in lunar soils. *Geochim. Cosmochim. Acta* **56**, 1025–1031.

Fryxell R. and Heiken G. H. (1974) Preservation of lunar core samples: Preparation and interpretation of three-dimensional stratigraphic section. *Proc. 5th Lunar Sci. Conf*. 935–966.

Galy A., Young E. D., Ash R. D. and O'Nions R. K. (2000) The formation of chondrules at high gas pressure in the solar nebula. *Science* **290**, 1751–1753.

Galy A., Yoffe O., Janney P. E., Williams R. W., Cloquet C., Alard O., Halicz L., Wadhwa M., Hutcheon I. D., Ramon E. and Carignan J. (2003) Magnesium isotope heterogeneity of the isotopic standard SRM980 and new reference materials for magnesium-isotope-ratio measurements. *J. Anal. At. Spectrom.* **18**, 1352–1356.

Giguere T. A., Taylor G. J., Hawke B. R. and Lucey P. G. (2000) The titanium contents of lunar mare basalts. *Meteorit. Planet. Sci.* **35**, 193–200.

Gillis J. J., Jolliff B. L. and Korotev R. L. (2004) Lunar surface geochemistry: Global concentrations of Th, K, and FeO as derived from lunar prospector and clementine data. *Geochim. Cosmochim. Acta* **68**, 3791–3805.

Greenhagen B. T., Lucey P. G., Wyatt M. B., Glotch T. D., Allen C. C., Arnold J. A., Bandfield J. L. and Bowles N. E. (2010) Global silicate mineralogy of the Moon from the Diviner lunar radiometer. *Science* **329**, 1507–1509.

Hallis L. J., Anand M., Greenwood R. C., Miller M. F., Franchi I. A. and Russell S. S. (2010) The oxygen isotope composition, petrology and geochemistry of mare basalts: Evidence for large-scale compositional variation in the lunar mantle. *Geochim. Cosmochim. Acta* **74**, 6885–6899.

Handler M. R., Baker J. A., Schiller M., Bennett V. C. and Yaxely G. M. (2009) Magnesium stable isotope composition of Earth's upper mantle. *Earth Planet. Sci. Lett.* **282**, 306–313.

Hartmann W. K. and Davis D. R. (1975) Satellite-sized planetesimals and lunar origin. *Icarus* **24**, 504–515.

Housley R. M. (1979) A model for chemical and isotopic fractionation in the lunar regolith by impact vaporization. *Proc. 10th Lunar Planet. Sci. Conf*. 1673–1683.

Huang F., Lundstrom C. C., Glessner J., Ianno A., Boudreau A., Li J., Ferré E. C., Marshak S. and DeFrates J. (2009) Chemical and isotopic fractionation of wet andesite in a temperature gradient: Experiments and models suggesting a new mechanism of magma differentiation. *Geochim. Cosmochim. Acta* **73**, 729–749.

Huang F., Zhang Z. F., Lundstrom C. C. and Zhi X. C. (2011) Iron and magnesium isotopic compositions of peridotite xenoliths from eastern China. *Geochim. Cosmochim. Acta* **75**, 3318–3334.

Humayun M. and Clayton R. N. (1995a) Precise determination of the isotopic composition of potassium: Application to terrestrial rocks and lunar soils. *Geochim. Cosmochim. Acta* **59**, 2115–2130.

Humayun M. and Clayton R. N. (1995b) Potassium isotope cosmochemistry: Genetic implications of volatile element depletion. *Geochim. Cosmochim. Acta* **59**, 2131–2148.

Jolliff B. L., Gillis J. J., Haskin L. A., Korotev R. L. and Wieczorek M. A. (2000) Major lunar crustal terranes: Surface expressions and crust mantle origin. *J. Geophys. Res.* **105**, 4197–4216.

Korotev R. L. and Morris R. V. (1993) Composition and maturity of Apollo 16 regolith core 60013/14. *Geochim. Cosmochim. Acta* **57**, 4813–4826.

Lee T., Papanastassiou D. A. and Wasserburg G. J. (1977) Aluminum-26 in the early solar system: Fossil or fuel? *Astrophys. J.* **211**, L107–L110.

Lee T., Russell W. A. and Wasserburg G. J. (1979) Ca isotopic anomalies and the lack of ^{26}Al in an unusual Allende inclusion. *Astrophys. J. Lett.*, L93–L98.

Li W.-Y., Teng F.-Z., Ke S., Rudnick R. L., Gao S., Wu F.-Y. and Chappell B. W. (2010) Heterogeneous magnesium isotopic composition of the upper continental crust. *Geochim. Cosmochim. Acta* **74**, 6867–6884.

Li W.-Y., Teng F.-Z., Xiao Y. and Huang J. (2011) High-temperature inter-mineral magnesium isotope fractionation in eclogite from the Dabie orogen, China. *Earth Planet. Sci. Lett.* **304**, 224–230.

Lind M. D. and Housley R. M. (1972) Crystallization studies of lunar igneous rocks: Crystal structure of synthetic armalcolite. *Science* **175**, 521–523.

Ling M.-X., Sedaghatpour F., Teng F.-Z., Hays P., Strauss J. and Sun W. (2011) Homogeneous magnesium isotopic composition of seawater: An excellent geostandard for Mg isotope analysis. *Rapid Commun. Mass Spectrom.* **25**, 2828–2836.

Liu Y., Spicuzza M. J., Craddock P. R., Day J. M. D., Valley J. W., Dauphas N. and Taylor L. A. (2010a) Oxygen and iron

isotope constraints on near-surface fractionation effects and the composition of lunar mare basalt source regions. *Geochim. Cosmochim. Acta* **74**, 6249–6262.

Liu S.-A., Teng F.-Z., He Y.-S., Ke S. and Li S.-G. (2010b) Investigation of magnesium isotope fractionation during granite differentiation: Implication for Mg isotopic composition of the continental crust. *Earth Planet. Sci. Lett.* **297**, 646–654.

Liu S.-A., Teng F.-Z., Yang W. and Wu F.-Y. (2011) High-temperature inter-mineral magnesium isotope fractionation in mantle xenoliths from the North China craton. *Earth Planet. Sci. Lett.* **308**, 131–140.

Lucey P., Korotev R. L., Gillis J. J., Taylor A., Lawrence D., Campbell B. A., Elphic Feldman B., Hood L. L., Hunten D., Mendillo M. R., Noble S., Papike J. J., Reedy R. C., Lawson S., Prettyman T., Gasnault O. and Maurice S. (2006) Understanding the lunar surface and space-moon interactions. *Rev. Mineral. Geochem.* **60**, 83–202.

Lodders K. (2003) Solar system abundances and condensation temperatures of the elements. *Astrophys. J.* **591**, 1220–1247.

Magna T., Wiechert U. and Halliday A. N. (2006) New constraints on the lithium isotope compositions of the Moon and terrestrial planets. *Earth Planet. Sci. Lett.* **243**, 336–353.

McKay D. S., Heiken G., Basu A., Blandford G., Simon S., Reedy R., French B. M. and Papike J. (1991) The lunar regolith. In *The Lunar Source Book Guide to the Moon* (eds. G. H. Heiken, D. T. Vaniman and B. M. French). Cambridge Univ. Press, pp. 285–356.

Meyer C. (2004–2011) Lunar sample compendium. Available from: <http://curator.isc.nasa.gov/lunar/compendium.cfm> and <http://www.lpi.usra.edu/lunar/samples>.

Morris R. V. (1978) The maturity of lunar soils: Concepts and more values of Is/FeO. *Lunar Planet. Sci. IX*. 760–762.

Morris R. V., Lauer Jr. H. V. and Gose W. A. (1979) Characterization and depositional and evolutionary history of the Apollo 17 deep drill core. *Proc. 10th Lunar Sci. Conf*. 1141–1157.

Morris R. V., Score R., Dardano C. and Heiken G. (1983). *Handbook of lunar soils-Part 2: Apollo 16–17*. NASA, Lyndon B. Johnson Space Center, p. 480.

Neal C. R. (2008) Mare basalt database. Available from: <http://www.nd.edu/~cneal/lunar-L/>.

Neal C. R. and Taylor L. A. (1992) Petrogenesis of mare basalts: A record of lunar volcanism. *Geochim. Cosmochim. Acta* **56**, 2177–2211.

Neal C. R., Hacker M. D., Snyder G. A., Taylor L. A., Liu Y.-G. and Schmitt R. A. (1994) Basalt generation at the Apollo 12 site, Part 1: New data, classification, and re-evaluation. *Meteoritics* **29**, 334–348.

Niederer F. R. and Papanastassiou D. A. (1984) Ca isotopes in refractory inclusions. *Geochim. Cosmochim. Acta* **48**, 1279–1293.

Niederer F. R., Papanastassiou D. A. and Wasserburg (1985) Absolute isotopic abundances of Ti in meteorites. *Geochim. Cosmochim. Acta* **49**, 835–851.

Norman M. D., Yaxley G. M., Bennett V. C. and Brandon A. D. (2006) Magnesium isotopic composition of olivine from the Earth, Mars, Moon, and Pallasite parent body. *Geophys. Res. Lett.* **33**, L15202.

Paniello R. C., Day J. M. D. and Moynier F. (2012) Zinc isotopic evidence for the origin of the Moon. *Nature* **490**, 376–379.

Pahlevan K. and Stevenson D. J. (2007) Equilibration in the aftermath of the lunar-forming giant impact. *Earth Planet. Sci. Lett.* **262**, 438–449.

Papike J. J., Ryder G. and Shearer C. K. (1998) Lunar samples. *Rev. Mineral. Geochem.* **36**, 1–234.

Pogge von Strandmann P. A. E., Elliott T., Marschall H. R., Coath C., Lai Y.-J., Jeffcoate A. B. and Ionov D. A. (2011) Variation of Li and Mg isotope ratios in bulk chondrites and mantle xenoliths. *Geochim. Cosmochim. Acta* **75**, 5247–5268.

Poitrasson F., Halliday A. N., Lee D. C., Levasseur S. and Teutsch N. (2004) Iron isotope differences between Earth, Moon, Mars and Vesta as possible records of contrasted accretion mechanisms. *Earth Planet. Sci. Lett.* **223**, 253–266.

Pritchard M. E. and Stevenson D. J. (2000) Thermal aspects of a lunar origin by giant impact. In *Origin of the Earth and Moon* (eds. R. Canup and K. Righter). University of Arizona Press, Tucson, pp. 179–196.

Raymond K. N. and Wenk H. R. (1971) Lunar ilmenite (Refinement of the crystal structure). *Contrib. Mineral. Petrol.* **30**, 135–140.

Rhodes J. M. and Blanchard D. P. (1982) Apollo 11 breccias and soils – Aluminous mare basalts or multi-component mixtures. *Proc. 12th Lunar Sci. Conf*. 607–620.

Richter F. M., Dauphas N. and Teng F.-Z. (2009a) Non-traditional fractionation of non-traditional isotopes: Evaporation, chemical diffusion and Soret diffusion. *Chem. Geol.* **258**, 92–103.

Richter F. M., Davis A. M., Ebel D. S. and Hashimoto A. (2002) Elemental and isotopic fractionation of Type B calcium-, aluminum-rich inclusions: Experiments, theoretical considerations, and constraints on their thermal evolution. *Geochim. Cosmochim. Acta* **66**, 521–540.

Richter F. M., Janney P. E., Mendybaev R. A., Davis A. M. and Wadhwa M. (2007) Elemental and isotopic fractionation of Type B CAI-like liquids by evaporation. *Geochim. Cosmochim. Acta* **71**, 5544–5564.

Richter F. M., Watson E. B., Mendybaev R., Dauphas N., Georg B., Watkins J. and Valley J. (2009b) Isotopic fractionation of the major elements of molten basalt by chemical and thermal diffusion. *Geochim. Cosmochim. Acta* **73**, 4250–4263.

Richter F. M., Watson E. B., Mendybaev R. A., Teng F.-Z. and Janney P. E. (2008) Magnesium isotope fractionation in silicate melts by chemical and thermal diffusion. *Geochim. Cosmochim. Acta* **72**, 206–220.

Russell W. A. and Papanastassiou D. A. (1978) Calcium isotope fractionation in ion-exchange chromatography. *Anal. Chem.* **50**, 1151–1154.

Russell W. A., Papanastassiou D. A., Tombrello T. A., and Epstein S. (1977) Ca isotope fractionation on the Moon. *Proc. 8th Lunar Sci. Conf*. 3791–3805.

Ryder G. and Schuraytz B. C. (2001) Chemical variation of the large Apollo 15 olivine-normative mare basalt rock samples. *J. Geophys. Rev.* **106**, 1435–1451.

Schauble E. A. (2011) First-principles estimates of equilibrium magnesium isotope fractionation in silicate, oxide, carbonate and hexaaqua magnesium (2+) crystals. *Geochim. Cosmochim. Acta* **75**, 844–869.

Schiller M., Handler M. R. and Baker J. A. (2010) High-precision Mg isotopic systematics of bulk chondrites. *Earth Planet. Sci. Lett.* **297**, 165–173.

Seitz H. M., Brey G. P., Weyer S., Durali S., Ott U., Münker C. and Mezger K. (2006) Lithium isotope compositions of Martian and lunar reservoirs. *Earth Planet. Sci. Lett.* **245**, 6–18.

Shearer C. K., Hess P. C., Wieczorek M. A., Pritchard M. E., Parmentier E. M., Borg L. E., Longhi J., Elkins-Tanton L. T., Neal C. R., Antonenko I., Canup R. M., Halliday A. N., Grove T. L., Hager B. H., Lee D.-C. and Wiechert U. (2006) Thermal and magmatic evolution of the Moon. *Rev. Mineral. Geochem.* **60**, 365–518.

Shearer C. K. and Papike J. J. (1993) Basaltic magmatism on the Moon: A perspective from volcanic picritic glass beads. *Geochim. Cosmochim. Acta* **57**, 4785–4812.

Shearer C. K. and Papike J. J. (1999) Magmatic evolution of the Moon. *Am. Mineral.* **84**, 1469–1494.

Snyder G. A., Taylor L. A. and Neal C. R. (1992) A chemical model for generating the sources of mare basalts: Combined equilibrium and fractional crystallization of the lunar magmasphere. *Geochim. Cosmochim. Acta* **56**, 3809–3823.

Spicuzza M. J., Day J. M. D., Taylor L. A. and Valley J. W. (2007) Oxygen isotope constraints on the origin and differentiation of the Moon. *Earth Planet. Sci. Lett.* **253**, 254–265.

Stöffler D., Knöll H. D., Marvin U. B., Simonds C. H. and Warren P. H. (1980) Recommended classification and nomenclature of lunar highland rocks. In: *Proc. Conf. Lunar Highland Crust*. Pergamon Press, New York and Oxford. pp. 51–70.

Switkowski Z. E., Haff P. K., Tombrello T. A. and Burnett D. S. (1977) Mass fractionation of the lunar surface by solar wind sputtering. *J. Geophys. Res.* **82**, 3797–3804.

Taylor S. R. (1982) *Planetary Science: A Lunar Perspective*. The Lunar and Planetary Inst, Houston.

Teng F.-Z., Dauphas N., Helz R. T., Gao S. and Huang S. (2011) Diffusion-driven magnesium and iron isotope fractionation in Hawaiian olivine. *Earth Planet. Sci. Lett.* **308**, 317–324.

Teng F.-Z., Li W.-Y., Ke S., Marty B., Dauphas N., Huang S., Wu F. Y. and Pourmand A. (2010) Magnesium isotopic composition of the Earth and chondrites. *Geochim. Cosmochim. Acta* **74**, 4150–4166.

Teng F.-Z., Wadhwa M. and Helz R. T. (2007) Investigation of magnesium isotope fractionation during basalt differentiation: Implications for a chondritic composition of the terrestrial mantle. *Earth Planet. Sci. Lett.* **261**, 84–92.

Urey H. C. (1947) The thermodynamic properties of isotopic substances. *J. Chem. Soc. (London)*, 562–581.

Van Kan Parker M., Mason P. R. D. and Van Westrenen W. (2011) Trace element partitioning between ilmenite, armalcolite and anhydrous silicate melt: Implications for the formation of lunar high-Ti mare basalts. *Geochim. Cosmochim. Acta* **75**, 4179–4193.

Wang S.-J., Teng F.-Z., Williams H. and Li S. (2012) Magnesium isotope variations in cratonic eclogites: Origins and implications. *Earth Planet. Sci. Lett.* **359–360**, 219–226.

Warner R. D., Nehru C. N. and Keil K. (1978) Opaque oxide mineral crystallization in lunar high-titanium mare basalts. *Am. Mineral.* **63**, 1209–1224.

Warren P. H. (1985) The magma ocean concept and lunar evolution. *Annu. Rev. Earth Planet. Sci.* **13**, 201–240.

Warren P. H. (2005) "New" lunar meteorites: Implication for composition of the global lunar surface, lunar crust and the bulk Moon. *Meteorit. Planet. Sci.* **40**, 477–506.

Warren P. H., Tonui E. and Young E. D. (2005) Magnesium isotopes in lunar rocks and glasses and implications for the origin of the Moon. *Lunar Planet. Sci. XXXVI*. Lunar Planet. Inst., Houston. #2143 (abstr.).

Wasserburg G. J., Lee T. and Papanastassiou D. A. (1977) Correlated O and Mg isotopic anomalies in Allende inclusions, II: Magnesium. *Geophys. Res. Lett.* **4**, 299–302.

Weber R. C., Lin P.-Y., Garnero E. J., Williams Q. and Lognonné P. (2011) Seismic detection of the lunar core. *Science* **331**, 309–312.

Weyer S., Anbar A. D., Brey G. P., Münker C., Mezger K. and Woodland A. B. (2005) Iron isotope fractionation during planetary differentiation. *Earth Planet. Sci. Lett.* **240**, 251–264.

Wiechert U. and Halliday A. N. (2007) Non-chondritic magnesium and the origins of the inner terrestrial planets. *Earth Planet. Sci. Lett.* **256**, 360–371.

Wiechert U., Halliday A. N., Lee D.-C., Snyder G. A., Taylor L. A. and Rumble D. (2001) Oxygen isotopes and the Moon-forming giant impact. *Science* **294**, 345–348.

Wieczorek M. A., Jolliff B. L., Khan A., Pritchard M. E., Weiss B. P., Williams J. G., Hood L. L., Righter K., Neal C. R., Shearer C. K., McCallum I. S., Tompkins S., Hawke B. R., Peterson C., Gillis J. J. and Bussey B. (2006) The constitution and structure of the lunar interior. *Rev. Mineral. Geochem.* **60**, 221–364.

Wiesli R. A., Beard B. L., Taylor L. A. and Johnson C. M. (2003) Space weathering processes on airless bodies: Fe isotope fractionation in the lunar regolith. *Earth Planet. Sci. Lett.* **216**, 457–465.

Xiao Y., Teng F.-Z., Zhang H.-F. and Yang W. (2013) Large magnesium isotope fractionation in peridotite xenolithis from eastern North China craton: Product of melt-rock interaction. *Geochim. Cosmochim. Acta* **115**, 241–261.

Yang W., Teng F.-Z. and Zhang H.-F. (2009) Chondritic magnesium isotopic composition of the terrestrial mantle: A case study of peridotite xenoliths from the North China craton. *Earth Planet. Sci. Lett.* **288**, 475–482.

Young E. D., Ash R. D., Galy A. and Belshaw N. S. (2002) Mg isotope heterogeneity in the Allende meteorite measured by UV laser ablation-MC-ICPMS and comparisons with O isotopes. *Geochim. Cosmochim. Acta* **66**, 683–698.

Young E. D. and Galy A. (2004) The isotope geochemistry and cosmochemistry of magnesium. *Rev. Mineral. Geochem.* **55**, 197–230.

Young E. D., Tonui E., Manning C. E., Schauble E. A. and Macris C. A. (2009) Spinel-olivine magnesium isotope thermometry in the mantle and implications for the Mg isotopic composition of Earth. *Earth Planet. Sci. Lett.* **288**, 524–533.

Associate editor: Dimitri A. Papanastassiou